ADVANCES IN SPACE DYNAMICS 4: CELESTIAL MECHANICS AND ASTRONAUTICS,
H. K. Kuga, Editor, 113-121 (2004).
Instituto Nacional de Pesquisas Espaciais – INPE, São José dos Campos, SP, Brazil.
ISBN 85-17-00012-9

A DESCRIPTION OF EXTRA-SOLAR PLANETARY ORBITS THROUGH A SCHRÖDINGER – TYPE DIFFUSION EQUATION

Marçal de Oliveira Neto
Instituto de Química – Universidade de Brasília
Campus Universitário – Asa Norte
70910-900 - Brasilia - DF - E-mail: marcal@unb.br
Liliane de Almeida Maia
Departamento de Matemática
Instituto de Ciências Exatas - Universidade de Brasília
Campus Universitário - Asa Norte
70910-900 - Brasília - DF - E-mail: lilimaia@unb.br
Saulo Carneiro
Instituto de Física
Universidade Federal da Bahia
40210-340 – Salvador – BA - E-mail: saulo@fis.ufba.br

ABSTRACT

The planetary orbits in our solar system have been successfully described by an approach similar to the Bohr atomic model [1-3]. A Schrödinger-type diffusion equation has shown that quantum states associated to the asteroid belt are in very good agreement with the observed mean radii of the asteroids which perform the internal and external orbits in the belt. According to these results, a model of quantum states condensation was proposed in order to infer the orbits of the planets in our solar system [4].

In this paper, the use of the Schrödinger-type diffusion equation reproduces the observed mean distances for the 101 extra-solar planets discovered up to now. A considerable number of these planets were found at the planetary mean distance of 0.05 AU from their stars, which is the fundamental radius obtained by this approach. Planets with mean distances of 2.0 AU were also predicted by the model.

A SCHRÖDINGER-TYPE EQUATION

A Schödinger-type equation in a disk arises when we employ quantum mechanics to describe a planar system involving an attractive central field, with a body of mass m moving around a body of mass M under an interaction potential $V(r)$:

$$-\frac{(g^*)^2}{2\mu}\left(\frac{\partial^2}{\partial r^2}\psi+\frac{1}{r}\frac{\partial\psi}{\partial r}+\frac{1}{r^2}\frac{\partial^2\psi}{\partial\theta^2}\right)+V(r)\psi=E_*\psi\,. \qquad (1)$$

The term in parenthesis is $\Delta\psi$, where Δ is the Laplace operator in polar coordinates, applied to a wave function ψ of the body of mass m, and μ is the reduced mass *mM/(m+M)*. The parameter E_* stands for the energy of the system and g^* is a constant with the dimension of the Planck constant.

As long as the potential V is a function of the radial variable only, we may look for a solution using separation of variables,

$$\psi(r,\theta)=f(r)\Theta(\theta)\,. \qquad (2)$$

Replacing (2) into (1) and dividing by $f(r)\Theta(\theta)$ we get:

$$\frac{1}{\Phi(\theta)}\frac{\partial^2\Phi(\theta)}{\partial\theta^2}=-\frac{r^2}{f(r)}\left(\frac{\partial^2 f}{\partial r^2}+\frac{1}{r}\frac{\partial f}{\partial r}\right)-\frac{2\mu}{(g^*)^2}r^2(E_*-V(r))\,.$$

Since the term on the left depends only on θ and the term of the right depends on r, both must be equal to a constant which we denote by $-\ell^2$.

Therefore we obtain two ordinary differential equations:

$$\frac{\partial^2\Theta(\theta)}{\partial\theta^2}=-\ell^2\Theta(\theta) \qquad (3)$$

and

$$\frac{\partial^2 f}{\partial r^2}+\frac{1}{r}\frac{\partial f}{\partial r}+\left[-\frac{\ell^2}{r^2}+\frac{2\mu}{(g^*)^2}(E_*-V(r))\right]f(r)=0\,. \qquad (4)$$

Equation (3) has a solution

$$\Theta(\theta)=e^{il\theta}\,.$$

If we assume the boundary conditions $\Theta(0)=\Theta(2\pi)$, we end up with $|\ell|=0,1,2,3,\cdots$, i.e., ℓ is an integer.

Now we apply a rescaling in (4) by

$$\rho=2\beta r \quad , \ \beta>0\,,$$

where $\beta^2=-\frac{2\mu E_*}{(g^*)^2}$. Furthermore, we define $\gamma=\frac{\mu GMm}{(g^*)^2\beta}$, and equation (4) becomes

$$\frac{\partial^2 \tilde{f}(\rho)}{\partial \rho^2} + \frac{1}{\rho}\frac{\partial \tilde{f}(\rho)}{\partial \rho} + \left(-\frac{1}{4} - \frac{\ell^2}{\rho^2} + \frac{\gamma}{\rho}\right)\tilde{f}(\rho) = 0. \qquad (5)$$

If we consider $\tilde{f}(\rho) = \frac{1}{\sqrt{\rho}}u(\rho)$ in (5) we obtain

$$u''(\rho) + \left\{-\frac{1}{4} + \frac{\gamma}{\rho} - \frac{(\ell^2 - 1/4)}{\rho^2}\right\}u(\rho) = 0. \qquad (6)$$

For this equation $\rho = 0$ is a regular singular point and $\rho = \infty$ is an irregular singular point. Equation (6) is a confluent hypergeometric equation, referred to as Whittaker's equation. This equation has a regular solution given by a hypergeometric series, which converges if, and only if,

$\gamma = |\ell| \pm \frac{1}{2} \pm k, \qquad k = 0,1,2,3\cdots$

By definition $\gamma \geq 0$ and, assuming that the solution $u(\rho)$ satisfy the boundary condition $\lim_{\rho \to +\infty} u(\rho) = 0$, and that $u(0)$ is finite, we must have

$$n = \gamma = |\ell| + \frac{1}{2} + k \ , \qquad k = 0,\ 1,\ 2,\ 3... \ ;\ \ell \text{ integer.}$$

So far we have the conditions

$$|\ell| = 0,\ 1,\ 2,\ 3,\ \ldots$$

$$n = \gamma = |\ell| + \frac{1}{2}, \quad |\ell| + \frac{3}{2}, \ |\ell| + \frac{5}{2}\ldots$$

They can be regrouped in the form

$$n = \frac{1}{2}, \frac{3}{2}, \frac{5}{2}, \frac{7}{2}, k$$

$$\ell = 0,1,\ 2,\ k\ , n - \frac{1}{2}$$

For each pair $n\ell$ the solutions $u_{n\ell}$ were obtained by using Maple V software. As long as we obtain $u_{n\ell}(\rho)$ we can recover the solution $f_{n\ell}(r)$ of the original equation (4). Once we know the collection of functions $f_{n\ell}(r)$ and $\Theta_\ell(r)$, their products generate the wave equations $\psi_{n\ell}$, solutions of the Schrödinger-type equation.

Now, we define $P_{n\ell}(r)dr = \int_0^{2\pi} \psi_{n\ell}^* \psi_{n\ell} r dr d\theta$, which is equivalent to $P_{n\ell}(r)dr = r\left[rf(r)\right]^2 dr.$

The mean radius is obtained by

$$\bar{r}_{n\ell} = \int_0^\infty rP_{n\ell}(r)dr = \int_0^\infty \int_0^{2\pi} (\psi_{n\ell}^* r \psi_{n\ell})\, r\, dr d\theta,$$

which is equivalent to

$$\bar{r}_{n\ell} = \int_0^\infty [r\, f(r)]^2\, dr. \qquad (7)$$

With these results, we now return to the rescaling factor β and consider the mean radius of the planet Mercury as $\bar{r}_{\frac{3}{2}0}$. (If we used $\bar{r}_{\frac{1}{2}0}$, all the set of results would be inconsistent with the observed mean planetary distances.) Under this assumption we obtain

$$\frac{1}{\sqrt{\rho}} u(\rho) = c_1 \left(- e^{-\frac{1}{2}\rho} + e^{-\frac{1}{2}\rho} \rho \right);$$

and $f(r) = c_1 e^{-\beta r} (2\beta r - 1)$. Since $\int_0^\infty [rf(r)]^2\, dr = 1$, we get

$$c_1 = \sqrt{\frac{4}{3}} \beta.$$

From Maple V calculations

$$\bar{r}_{\frac{3}{2}0} = \frac{7}{3} \cdot \frac{1}{\beta} = 0.387,$$

and we obtain

$$\beta = \frac{1}{0.387} \cdot \frac{7}{3} = 9.043927648 / (3/2).$$

Therefore, we will consider, in each case,

$$\beta = \beta_n = 9.043927648(1/n) .$$

RESULTS AND DISCUSSIONS

Table I shows the theoretical planetary radii calculated from the states associated to the pairs (***n,l***), from the fundamental radius until the value corresponding to Jupiter. These theoretical values were considered as reference states to those found for the observed distances in the investigated extra-solar systems.

In Table II the studied stars, the semi-major axis distances of the planets and respective eccentricities are presented as described in Schneider's Extra-Solar Catalog [5]. The stars which masses are not yet known, were not taken into account. Therefore, 91 planets among a total of 101 discovered up to the present were investigated in this study. The table also shows the mean distances calculated from the average of the semi-major and semi-minor axis, the later obtained from the observed eccentricities. In the last column it is presented the rescaled mean radii derived from the relation $MR = M_0R_0$, where R_0 is the average between the major and minor axis, M_0 is the star mass, and R is the resulting rescaled

radius, calculated assuming the star mass M as equal to the solar mass. This relation was obtained from our previous theoretical studies [1,4,6].

Tables III and IV show the frequency of coincidence between the rescaled extra-solar mean radii and our theoretical reference states, as obtained from the solutions of the diffusion equation. It was considered an error of 10% and 15% below and above the reference states in the combined observed and theoretical numerical calculations. Figures I and II present the resulting graphics obtained from Tables III and IV, showing the frequency in which the observed extra-solar mean radii coincide with the theoretical results. In these figures the observed semi-major axis were also shown, for the purpose of comparing their frequencies with those calculated from the rescaled radii.

The results show a very satisfactory agreement with the observed values, except those with mean radius at 0.15 AU, 0.25 AU and 0.5 AU. However, theoretical calculations based on a Bohr-like model [1,4] can show that bodies may be found at 0.18 AU, which is approximately the mean distance between 0.15 AU and 0.25 AU. Mean distances at 0.5 AU could not be predicted neither from a Bohr-like model nor from the solutions of the Schrödinger-type diffusion equation.

It is interesting to note that the most frequent observed mean distances were those associated to the fundamental radius at 0.05 AU, to the Earth radius at 1 AU, and to the belt asteroids from 2.49 AU to 3.37 AU.

Table I - Theoretical mean radii $\bar{r}_{nl}$ obtained by the model

POSITION	**GRAPHIC NOTATION**	**PAIRS (*n,l*)**	**CALCULATED MEAN RADIUS (AU)**
Fundamental Radius	FR	(1/2,0)	0,055
Mercury	MER	(3/2,0) (3/2,1)	0,387; 0,332
Venus	VEN	(5/2,2)	0,83
Earth	EAR	(5/2,0); (5/2,1)	1,05; 0,995
Mars	MAR	(7/2,3)	1,54
Hungarian	HUN	(7/2,0); (7/2,1); (7/2,2)	2,04; 1,99; 1,82
Asteroid Belt	BELT	(9/2,0); (9/2,1); (9/2,2); (9/2,3) (9/2,4)	3,37; 3,32; 3,15; 2,88; 2,49
Jupiter	JUP	(11/3,3) to (13/2,4)	4,53 to 6,13

Table II - Extra-Solar Planets Data

STAR	**SEMI_MAJ**	**ECC**	**MEAN RADIUS**	**STAR MASS**	**RESCALED RADIUS**
HD 49674	0,0568	0	0,0568	1	0,0568
HD 76700	0,049	0	0,049	1,05	0,05145
HD 16141	0,35	0,28	0,343	1,1	0,3773
HD 168746	0,065	0,081	0,064893208	0,92	0,059701752
HD 46375	0,041	0	0,041	1	0,041
HD 83443	0,038	0,08	0,037939102	0,79	0,029971891
HD 108147	0,104	0,498	0,097093206	1,27	0,123308371

HD 75289	0,046	0,054	0,045966442	1,05	0,048264764
51 PEG	0,05	0	0,05	1	0,05
BD-10 3166	0,046	0	0,046	1,1	0,0506
HD 6434	0,15	0,3	0,14654544	1	0,14654544
HD 187123	0,042	0,03	0,041990548	1,06	0,044509981
HD 209458	0,045	0	0,045	1,05	0,04725
Ups And	0,059	0,034	0,058982944	1,3	0,076677827
Ups And	0,83	0,18	0,823221643	1,3	1,070188136
Ups And	2,5	0,41	2,390106903	1,3	3,107138974
Epsilon Eridani	3,3	0,608	2,959996092	0,8	2,367996873
HD 38529	0,12	0,312	0,117004926	1,39	0,162636847
HD 38529	3,51	0,34	3,40544664	1,39	4,733570829
HD 4208	1,69	0,04	1,689323729	0,93	1,571071068
HD 179949	0,045	0,05	0,044971857	1,24	0,055765103
55 Cnc	0,11	0,03	0,109975244	1,03	0,113274502
55 Cnc	6,01	0,16	5,971286628	1,03	6,150425227
HD 82943	0,73	0,54	0,672207731	1,05	0,705818118
HD 82943	1,16	0,41	1,109009603	1,05	1,164460083
HD 121504	0,32	0,13	0,318642239	1	0,318642239
HD 114783	1,2	0,1	1,196992462	0,92	1,101233065
HD 114729	2,08	0,33	2,021740169	0,93	1,880218357
HD 37124	0,585	0,1	0,583533825	0,91	0,531015781
HD 37124	2,95	0,4	2,82685983	0,91	2,572442445
HD 147513	1,26	0,52	1,168124744	0,92	1,074674764
HD 130322	0,088	0,048	0,087949283	0,79	0,069479933
rho CrB	0,23	0,028	0,229954911	0,95	0,218457166
HD 52265	0,49	0,29	0,479471528	1,13	0,541802827
G1 777A	3,65	0	3,65	0,9	3,285
HD 223084	0,41	0,48	0,38484004	1,05	0,404082042
HD 177830	1	0,43	0,951414444	1,17	1,113154899
HD 217107	0,07	0,14	0,069655303	0,98	0,068262197
HD 210277	1,097	0,45	1,038326162	0,99	1,027942901
HD 142	0,98	0,37	0,945225559	1,1	1,039748115
HD 27442	1,18	0,02	1,179881988	1,2	1,415858386
16 CygB	1,7	0,67	1,481006933	1,01	1,495817003
HD 74156	0,276	0,649	0,2429888	1,05	0,25513824
HD 74156	4,47	0,395	4,288252303	1,05	4,502664918
HD 134987	0,78	0,25	0,767615876	1,05	0,80599667
HD 4203	1,09	0,53	1,007158715	1,06	1,067588237
HD 108874	1,07	0,2	1,059190805	1	1,059190805
HD 68988	0,071	0,14	0,070650378	1,2	0,084780454
HD 160691	1,5	0,31	1,463052417	1,08	1,580096611
HD 19994	1,3	0,2	1,286867333	1,35	1,7372709
HD 216437	2,7	0,34	2,619574338	1,07	2,802944542

Gliese 876	0,21	0,27	0,206100334	0,32	0,065952107
Gliese 876	0,13	0,12	0,129530303	0,32	0,041449697
47 Uma	2,1	0,096	2,095150401	1,03	2,158004913
47 Uma	3,73	0,1	3,72065157	1,03	3,832271117
HD 12661	0,85	0,347	0,82359268	1,07	0,881244167
HD 12661	2,61	0,22	2,578027333	1,07	2,758489246
HD 72659	3,24	0,18	3,213539909	0,95	3,052862913
HD 128311	1,06	0,21	1,048181735	0,8	0,838545388
HD 169830	0,823	0,34	0,798485067	1,4	1,117879093
HD 196050	2,5	0,28	2,45	1,1	2,695
HD 73526	0,66	0,34	0,640340394	1,02	0,653147202
HD 40979	0,818	0,42	0,780177359	1,08	0,842591547
14 Her	2,5	0,3537	2,419198651	0,79	1,911166934
GJ 3021	0,49	0,505	0,456464239	0,9	0,410817815
HD 80606	0,439	0,927	0,301825962	0,9	0,271643365
HD 195019	0,14	0,05	0,139912445	1,02	0,142710694
HD 92788	0,94	0,36	0,908487582	1,06	0,962996837
Tau Boo	0,0462	0,018	0,046196257	1,3	0,060055135
Gl 86	0,11	0,046	0,109941779	0,79	0,086854006
HD 213240	2,03	0,45	1,921423983	1,22	2,34413726
HD 50554	2,38	0,42	2,269953684	1,1	2,496949053
HD 190228	2,31	0,43	2,197767365	1,3	2,857097574
HD 2039	2,2	0,69	1,896190304	0,98	1,858266498
HD 222582	1,35	0,71	1,150336131	1	1,150336131
HD 28185	1	0,06	0,999099189	0,99	0,989108197
HD 178911	0,32	0,1243	0,318759149	0,87	0,27732046
HD 10697	2	0,12	1,992773892	1,1	2,192051281
70 Vir	0,43	0,4	0,412050755	1,1	0,45325583
HD 106252	2,61	0,54	2,403372847	1,05	2,523541489
HD 89744	0,88	0,7	0,754222851	1,4	1,055911991
HD 30177	2,6	0,22	2,568149833	0,95	2,439742342
HD 168443	0,29	0,529	0,268050164	1,01	0,270730666
HD 168443	2,85	0,228	2,812467113	1,01	2,840591784
HD 33636	2,62	0,39	2,516267462	0,99	2,491104787
HIP 75458	1,34	0,71	1,141815123	1,05	1,198905879
HD 141937	1,52	0,41	1,453184997	1	1,453184997
HD 39091	3,34	0,62	2,980285022	1,1	3,278313525
HD 114762	0,3	0,334	0,291385961	0,82	0,238936488
HD 136118	2,335	0,366	2,253992838	1,24	2,794951119
HD 162020	0,072	0,277	0,070591317	0,7	0,049413922

Table III – Number of rescaled mean radii which coincide with those calculated by the model within an error of 10% .

	Radii	Semi-Maj.
FR	7	3
Mer	4	5
Ven	4	6
Ear	13	8
Mar	5	3
Hun	6	7
Belt	17	18
Jup	3	2
Total	59	52

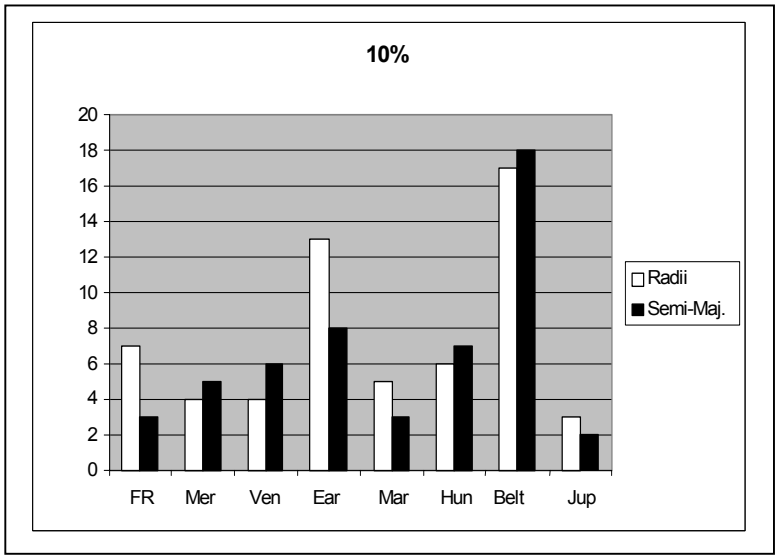

Figure I – Frequency of rescaled mean radii and semi-major axis that coincide with those calculated by the model within an error of 10%.

Table IV– Number of rescaled mean radii which coincide with those calculated by the model within na error of 15%.

	Radii	Semi-Maj.
FR	10	4
Mer	4	8
Ven	5	8
Ear	16	13
Mar	6	6
Hun	8	8
Belt	20	20
Jup	3	2
Total	72	69

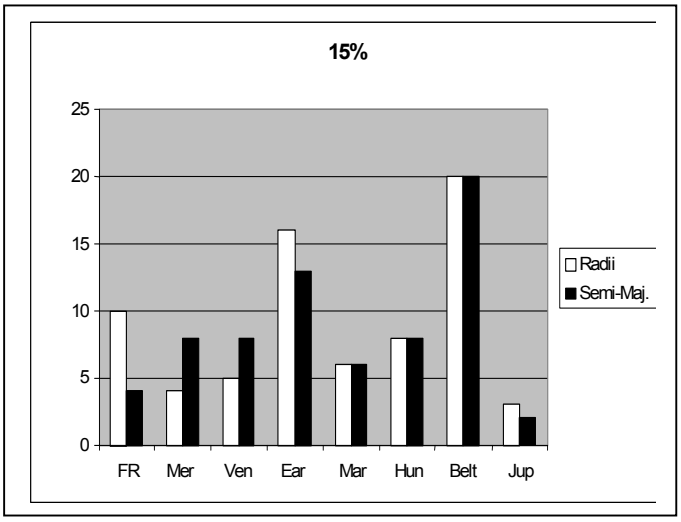

Figure II – Frequency of rescaled mean radii and semi-major axis that coincide with those calculated by the model within an error of 15%.

For larger values of n, a great number of states is found [6]. However, for extra-solar systems no orbits were yet discovered beyond Jupiter's radius. In the case of our Solar System, as pointed out by Nottale et al. [2] to explain the circularity of the orbits, a great number of states occupying the same region of space, most of them with large eccentricities, leads to a strong chaos and to the crossing of orbits, which on large time scales could generate the condensation of states on the observed, approximately circular orbits. Therefore, for $n > 9/2$ we will consider only the states with rotational symmetry, that is, with $l = 0$.

If we denote by the triple (*n, l, r*) the resulting numbers *n, l* and the corresponding mean planetary radius r_{nl} (in AU), then the states (11/2,0,5.03) and (15/2,0,9.34) can be associated with the orbits of Jupiter and Saturn, respectively. The states (17/2,0,12.0) and (19/2,0,15.0) give mean values around the orbit of the asteroid Chiron, distant 13.7 AU from the Sun. The states (21/2,0,18.3) can be associated with the orbit of Uranus, while the states (25/2,0,25.9) has a mean distance close to the orbital radii of the recently discovered asteroids 1993 HA 2 and 1995 DW 2. The next state, (27/2,0,30.2), clearly stands for the orbit of Neptune and, finally, the states (31/2,0,39.9) can easily be associated with the orbit of Pluto.

CONCLUSIONS

Theoretical results for the extra-solar planetary systems show a great coincidence between the planet distances and the radii corresponding to the fundamental state, to the Earth and to the Asteroid Belt, after the performing of a rescaling of distances, considering the different stellar masses. Some observed radii do not coincide with the radii obtained by the flat solutions of the Schrödinger-type equation. This could be due either to the tri-dimensional nature of the corresponding systems or to uncertainty in the present observations.

In the case of our solar system, the theoretical results show very good agreement with the exterior orbits when only states with rotational symmetry ($l = 0$) are taken into account.

REFERENCES

1 M. Oliveira Neto, Ciência e Cultura (Journal of the Brazilian Association for the Advancement of Science), 48 (1996) 166.

2 L. Nottale, G. Schumacher and J. Gay, A&A, 332 (1997) 1018.

3 A. G. Agnese and R. Festa, Phys. Lett. A, 227 (1997) 165.

4 M. Oliveira Neto and L.A. Maia, *Advances in Space Dynamics*, A. F. Bertachini, Editor, pp 456-470 (2000).

5 http://www.obspm.fr/encycl/catalog.html.

6 M. Oliveira Neto, L. A. Maia and S. Carneiro, astro-ph/0205379.